Indian Journal of Engineering & Materials Sciences
Vol. 29, December 2022, pp. 714-722
DOI: 10.56042/ijems.v29i6.70290

Modeling of Dry Conditioned Sliding Wear And Friction Behavior of Heat-Treated Silicon Nitride Strengthened Al Metal Matrix Nanocomposites

Ashish Kumar[a*], Ravindra Singh Rana[a], Rajesh Purohit[a], & Soni Kumari[b]

[a]Department of Mechanical Engineering, Maulana Azad National Institute of Technology, Bhopal 462 003, India
[b]Department of Mechanical Engineering, GLA University, Mathura 281 406, India

Received: 9 September 2022; Accepted: 17 October 2022

In the presented work, the sliding wear under dry conditions and friction behaviour of Si_3N_4 reinforced high-strength Aluminum alloy (AA)7068 nanocomposites have been investigated under various loads, sliding velocity, and rubbing distances. The fabrication of nanocomposites has been done by using the stir casting technique with the advancement of ultrasonication. Scanning electron microscope (SEM), Elemental mapping, and energy dispersive spectroscopy (EDS) are used to analyze the microstructure of prepared nanocomposites and worn surfaces. The wear resistance improves with the incorporation of Si_3N_4 particles in Al 7068 alloy and further increases by increasing the weight % of reinforcement. The reinforcement is done by 0.5, 1, and 1.5 % Si_3N_4 by weight. ANOVA reveals that sliding distance is the most dominating factor in the wear loss of samples, and load became the most influential parameter in the coefficient of friction (COF). Microstructure reveals grain boundaries become discontinued after T6 heat treatment. AMNCs containing 1.5wt.% Si_3N_4 shows minimum wear loss compared to other nanocomposites and alloys.

Keywords: Aluminum metal matrix nanocomposites, T6 heat treatment, Microstructure, Sliding wear, Friction, Design of Experiment

1 Introduction

The world is undergoing a revolution of electric vehicles, so the demand for light and strong automotive parts applications increased. Aluminium metal matrix nanocomposites (AMNCs) are the best option to replace traditional materials. AMNCs possess a very high strength-to-weight ratio, excellent strength, resistance to corrosion, and high stiffness, making them suitable for automotive, aerospace, and structural applications. Several existing methods to fabricate AMNCs include powder metallurgy[1], stir casting[2], in-situ method [3], friction stir welding, compo casting[4], chemical vapour deposition method[5] etc. Al alloy could be strengthened by ceramic particle incorporation to increase its strength and tribological properties. The reinforcement can be done by ceramic particles such as SiC[6], B_4C[7], Al_2O3[8], TiO_2[1], TiB_2[9], Si_3N_4[10], etc., to improve the wear strength of the composite.

Mohanavel Vet al.[11] fabricated the Al-mg-Si (6061)/Si_3N_4 composites at different weight percentages through a stir casting approach and performed a wear test to investigate the tribological characteristics. They found the wear resistance increased steadily by introducing Si_3N_4 particles in the matrix, and minimum wear was noticed at 3wt.% composite. Bhuvanesh D et al.[12] fabricated LM24/ Si_3N_4 composite using the stir casting method and optimized the wear parameters by the Taguchi method. They found load is the most dominating factor on wear loss, sliding velocity is the second most dominating, and sliding distance is the minor influential parameter on wear response. Raj N et al.[13] prepared 13% Si_3N_4 and 3% Gr reinforced LM13 composite via liquid metallurgy route. They investigated the tribological behaviour of composite and alloy at various loads (10N, 20N, and 30N), sliding velocity (1m/s, 2m/s and 3m/s and sliding distance (750m, 1250m, and 1750m), and quoted COF decrease with increase in load, sliding distance and load are most influential parameters on wear rate and COF. Mistry J M et al.[14] researched 7075/Si_3N_4 composite where reinforcement was done by 4wt.%, 8wt.%, and 12wt.% in 7075 matrices. Tribological characteristics of the composite were analyzed at various sliding velocities, loads, and sliding distances. They found wear loss reduced with an increase in sliding velocity, while wear loss

*Correspondence author
(E-mail: rpurohit73@gmail.com)

improves with an increase in rubbing distance and applied load.Sharma N et al.[15] developed Al6061/ Si_3N_4 + nano graphite (Gr) composite through stir casting approach; Gr varies from 3-15 wt.%. They used the DOE tool to analyze the wear behaviour of composites; results have shown that sliding distance is the most dominating factor followed by applied load and rubbing velocity. Stalin B et al.[16] fabricated Al6063/ Si_3N_4 composite using a liquid metallurgy approach; authors conducted the wear test on a tribometer, and wear parameters were optimized using Taguchi grey analysis method. They collectively found 29.43N load, 3m/s velocity, and 10wt% as the optimum set of parameters to get the minimum wear loss.

Alipour Met al.[17] prepared AA7068/GNP nanocomposite using stir casting method and compared mechanical and tribological properties under as-cast and heat-treated conditions. They noticed a reduction in wear loss after heat treatment for alloy and nanocomposites, and COF decreased after the addition of GNP and heat treatment. Abrasive wear mechanism more dominant during wear test revealed by worn surface images. [1] use powder metallurgy technique to fabricate AA7068/TiO_2 nanocomposites; the reinforcement is done by 3wt.%, 6wt.%, and 9wt.% in the matrix. They performed a wear test and found that delamination, abrasion, and oxidation are the most effective wear mechanism. The hardness of the alloy was tremendously enhanced by adding nano reinforcement and maximizing at 9wt.%.

From the literature survey, it is observed that much research has been done on the effect of nanoparticle reinforcement in the Al matrix on tribological and microstructural properties. Nevertheless, the tribological behaviour of AA 7068 matrix-based composites reinforced with nanosized Si_3N_4 was examined. So current study deals with the fabrication of AA7068/Si3N4 nanocomposites with varying weight % of reinforcement using ultrasonic assisted stir casting. Later the microstructural evolution has been investigated. for tribological properties analysis,a dry sliding wear test has been performed using different process parameters and optimization of the wear parameter was done using the Taguchi approach.

2 Materials and Methods

2.1 Materials

zinc-rich AA7068 alloy used as matrix material. The major alloying elements of alloy are Zn (7.6 %), Mg (3.1 %), and Cu (2.2 %), followed by Si (0.17 %) and Fe (0.13 %). Alloy is purchased from paraswamani metals Mumbai, in the form of ingots. Hard ceramic Si_3N_4 nanoparticles are used as reinforcement to increase the wear properties of the alloy, the size of Si_3N_4 in the range of 20nm to 86nm (average 54.16nm). Si_3N_4 particles are procured from Nano research element, India. Elemental mapping of Si_3N_4 identified the Si and N elements (shown in Fig. 1).

2.2 Fabrication of AMNCs

Fabrication of AMNCs is done in two steps. Initially, a planetary ball milling machine mixed 150gm silicon nitride (Si_3N_4) nanopowder and 450gm pure aluminum powder (Amaze instrument; ISO 9001:2015, Noida) for 2h. Stainless steel jars (capacity 500ml) and steel balls of diameter 10mm

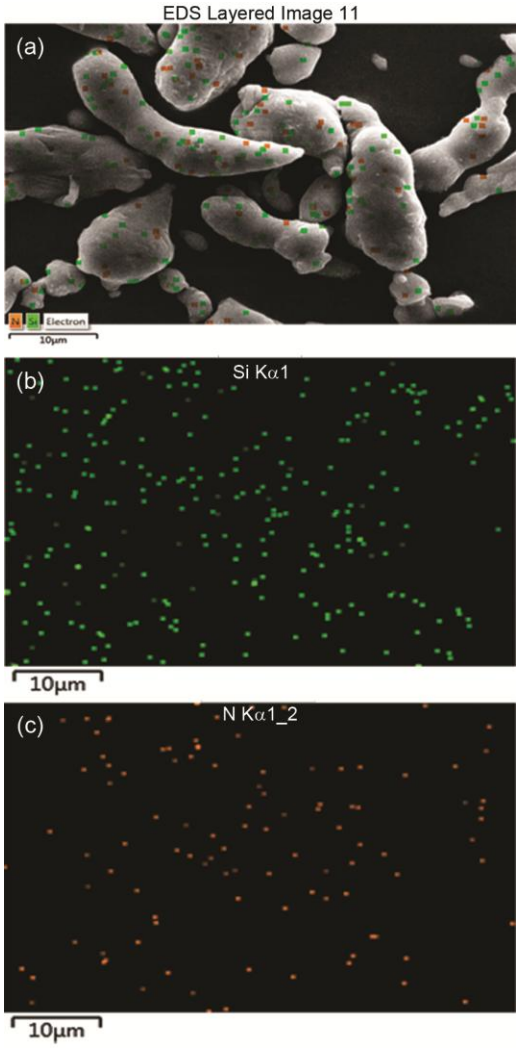

Fig. 1 (a-c) — Elemental Mapping of Si_3N_4 powder.

were used in the milling process. It is considered that jars are filled with 2/3rd of their maximum capacity to ensure efficient mixing. The mixture of Si_3N_4 and Al powder was compacted under the pressure of 450 MPa and made capsules of it.

The next step is casting AMNCs using stir casting with the ultrasonic application method (shown in Fig. 2). Al 7068 bars are loaded in a graphite crucible and melted at 760ºC in an electric resistance furnace. 1 wt.% coverall -11 was mixed into molten metal to remove its impurities. The preheat treatment of steel molds and mixed powder was performed at 350ºC with a soaking time of 30minutes. After removing impurities, compacted capsules of reinforcement were added to the molten metal in two steps with the continuation of the stirring process. Stirring was performed using a steel stirrer in which blades are fixed at 45º orientation with the horizontal plane. After proper mixing, ultrasonic vibration of frequency 2Hz was transmitted into the slurry with the help of a niobium probe to break the cluster of particles for 5 minutes. Finally, the prepared slurry was poured into preheated permanent molds.

Samples are prepared after solidification of each casting under ASTM guidelines; T6 heat treatment was performed on prepared specimens to alter theproperties of AMNCs. There are two steps in T6 treatment, where solutionizing is followed by artificial aging. Initially, Solution treatment, where samples were heated at 450ºC with the soaking time of 6h, then quenched in the water (at room temperature). Solution-treated samples were artificially aged, where samples were heated at 180ºC with the soaking time of 8h followed by air cooling.

There are four compositions are fabricated in which one is unreinforced alloy and three are composites. The unique designation are given to compositions such as HC-1 for pure 7068 alloy, HC-2 for AA7068/Si_3N_4 (0.5 wt. %), and HC-3 for AA7068/Si_3N_4 (1.0 wt. %), and HC-4 for AA7068/ Si_3N_4 (1.5 wt. %).

Cylindrical pins for all compositions (10mmx30mm) were machined after T6 heat treatment to conduct the wear test. The dry conditioned sliding test was performed on a pin-on-disc machine (DUCOM, India); EN-31 disc of 120mm diameter and 30mm thickness was used against AMNCs specimens. Electronic balance with 0.001mg precision was used to measure the weight of wear samples before and after the wear test. The Surface morphology of casted and worn surfaces was analyzed using a Scanning electron microscope (SEM) at maintained 20 Kv accelerating voltage and 9.5mm working distance. EDS and elemental mapping were carried out to study the elemental information of alloy and nanocomposites. Above mentioned facilities are used in IIT Kanpur and performed on CARL ZEISS EVO 50.

2.3 Design of Experiments

The wear calculation is done by calculating the weight difference before and after the wear test. The sliding wear was performed on a rotary tribometer under dry conditions and précised electronic balance was used to calculate weight difference in milligrams. Three levels of wear controlling factors such as sliding velocity (1.047, 2.094, and 3.141m/s), slidingdistance (800, 1600, and 2400), and normal

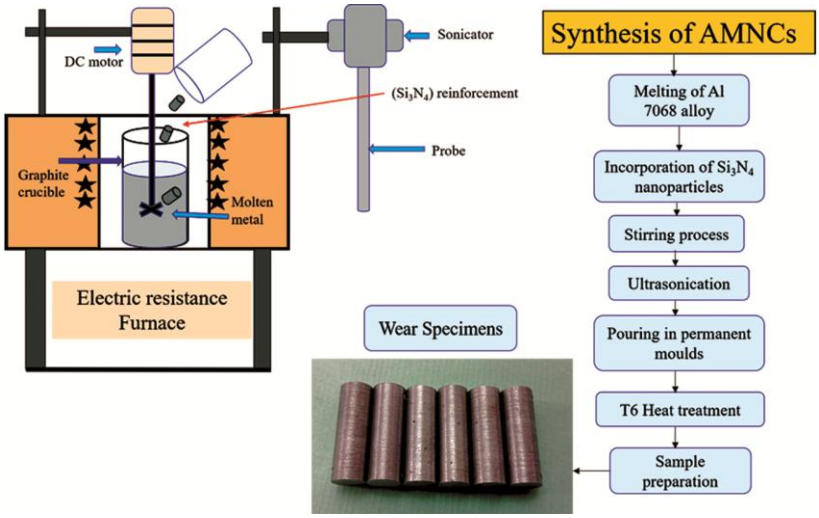

Fig. 2 — Stir casting with ultrasonic treatment schematic view.

load (15, 30, and 45N). The analysis of wear and friction behavior was done for Al 7068 alloy (HC-1), 0.5 wt.% (HC-2), 1 wt.% (HC-3), and 1.5 wt.% (HC-4) at thevarious combination of controlling parameters. Taguchi method was used to analyze the wear and frictional co-efficient responses. Initially, a three-level design with three controlling parameters was chosen to create Taguchi L-9 design matrix (shown in Table 1). The wear and frictional co-efficient responses were obtained by performing a wear test on a set of parameters provided by the L-9 matrix. After analyzing the responses, theregression tool was used to know the response variation in percentage and get an equation for predicting wear and frictional co-efficient for all compositions. ANOVA tool was used to know the percentage contribution of process parameters.

3 Results and Discussion

3.1 Microstructure study

Figure 3 (a) shows the microstructure of as-cast AA7068 and Fig. 3 (b-d) are the microstructure of

Table 1 — L9 Taguchi matrix with results

S. No	Experiment No.	Sliding velocity (m/s)	Load (N)	Rubbing Distance (m)	Wear of HC-1 (grams)	Wear of HC-2 (grams)	Wear of HC-3 (grams)	Wear of HC-4 (grams)	COF (HC-1)	COF (HC-2)	COF (HC-3)	COF (HC-4)
1	1	1.047	15	800	0.0056	0.0047	0.0039	0.0033	0.54	0.52	0.50	0.51
2	2	1.047	30	1600	0.0075	0.0069	0.006	0.0053	0.47	0.46	0.43	0.44
3	3	1.047	45	2400	0.0098	0.0085	0.0074	0.0067	0.45	0.44	0.41	0.40
4	4	2.094	15	1600	0.0064	0.0057	0.0045	0.0038	0.57	0.53	0.52	0.47
5	5	2.094	30	2400	0.0083	0.0076	0.0062	0.0054	0.46	0.45	0.42	0.43
6	6	2.094	45	800	0.0072	0.0062	0.0051	0.0046	0.41	0.40	0.37	0.33
7	7	3.141	15	2400	0.0071	0.0059	0.0053	0.0048	0.54	0.51	0.49	0.45
8	8	3.141	30	800	0.0061	0.0047	0.0036	0.0031	0.41	0.41	0.37	0.38
9	9	3.141	45	1600	0.0066	0.006	0.0045	0.0036	0.39	0.38	0.38	0.37
	Average value				**0.0072**	**0.0062**	**0.0052**	**0.0045**	**0.471**	**0.456**	**0.432**	**0.420**

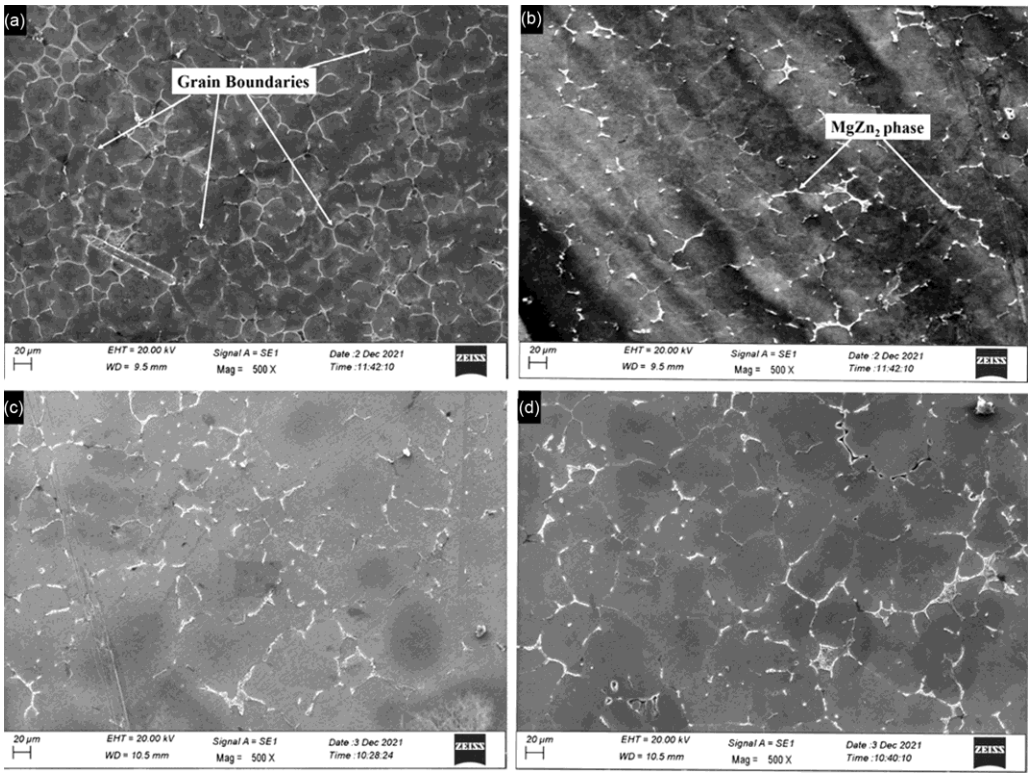

Fig. 3 — SEM micrographs of (a) HC-1 as cast condition, (b) HC-1 after heat treatment, (c) HC-2 after heat treatment, (d)) HC-3 after heat treatment, and (e)) HC-4 after heat treatment.

heat-treated alloy (HC-1) and nanocomposites (HC-2, and HC-4). Continuous grain boundaries observed in the case of as-cast alloy, these boundaries discontinue after performance of T6 heat treatment. Bright eutectic intermetallic phases of $MgZn_2$, Al_2Cu, and Al_2CuMg were observed at the grain boundaries of as-cast alloy. These phases dissolved during solution treatment and distributed uniformly during artificial aging. Precipitations of $MgZn_2$ were obtained after T6 heat treatment. The refinement in grain size was also noticed with the incorporation of nano Si_3N_4; the grain boundaries increased by T6 treatment and nanoparticleinsertion. The grains size became smaller with increasing Si_3N_4 wt.% in matrix alloy due to the presence of hard Si_3N_4 particles as a hindrance to grain growth during solidification. Microstructure identifies thepresence of Si_3N_4 and its homogeneous distribution throughout the matrix alloy.

3.2 Tribological characteristics

The sliding wear and friction behaviour of HC-1, HC-2, HC-3, and HC-4 was analyzed by conducting a wear test on a rotary tribometer (pin-on-disc). Various sliding velocities, loads, and rubbing distances with different levels are considered to understand nanocomposites' friction and wear behaviour. Further ANOVA andregression tools were used to find each factor's percentage contribution and variation in wear and frictional co-efficient response.

3.3 Effect of reinforcement on wear loss

The effect of reinforcing content in AA 7068 alloy on wear loss for each experiment is displayed in Table 1; wear loss seems to decrease with increasing Si_3N_4wt. %. The Si_3N_4 reinforcement in AA7068 is done in the proportions of 0, 0.5, 1 and 1.5% designated as HC-1, HC-2, HC-3 and HC-4 respectively. The average value of weight loss for HC-1, HC-2, HC-3 and HC-4 are 0.0072, 0.0062, 0.0052 and 0.0045 gms respectively. Wear resistance improves as the ceramic reinforcement increases in the pure alloy. From the experimental results, wear loss was minimized by 13.88%, 27.78% and 37.5% for 0.5%, 1% and 1.5% Si_3N_4 respectively. The decrement in wear with the inclusion of reinforcement is mainly due to the hard nature of ceramicSi_3N_4 reinforcement; when present in soft Al alloy, resists the plastic deformation of material during shear loading. The Oxide layer formation also contributes to the improvement of wear resistance. These layers are formed during the rubbing action ofthe specimen over the hard disc. Also, these are known as the mechanically mixed layer (MML) or tribo-chemical layer. The tendency to formation of MML increases with weight percentage increment. Due to the presence of MML between pin and disc, the actual Contact between specimen and disc gets affected, resulting in minimizing wear loss [18].

3.4 Effect of operating factors on wear

The operating parameters for the wear test are load, sliding/rubbing velocity, and sliding/rubbing distance. Main effect plots(MEP) could understand the impact of these parameters on wear loss for 1.5 wt. % (HC-4) composite (shown in Fig. (a)).With the increment of load, increasing wear loss was noticed, this behavioris credited to the fact that the material undergoes plastic deformation with the application of normal load. The tendency of plastic deformation increases at higher load due to sub-cracking of surface[19]. Sliding velocity also plays a critical role in wear loss. The wear loss decreased with increasing sliding velocity from Fig. 5 (a). The velocity increment directly affects the wear of the sample due to excessive heating at the interface; the generation of heat exceeds the tendency of MML formation and the rich tribo-chemical layer formedbetween pin and disc. MML

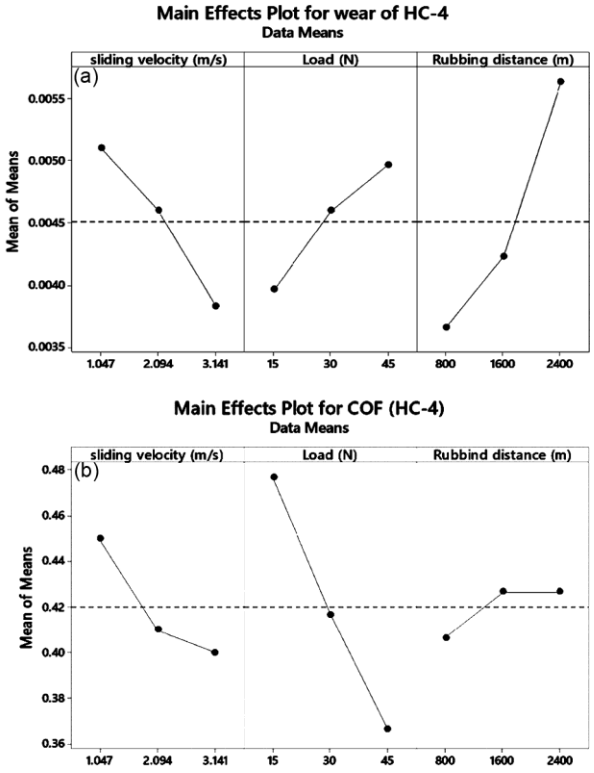

Fig. 4 — MEPs for (a) wear, and (b) frictional co-efficient.

decreases the actual contact area of the pin to disc; results wear loss decreases. The effect of Sliding/ rubbing distance on wear loss could be understood from the MEP plot. Increasing wear loss was noticed when samples were slid against hard disc for prolong period. Whereas, in the case of nanocomposites, the bonding between reinforcement and matrix gets affected when increasing in sliding distance. Analysis of variance (ANOVA) for wear loss for 1.5 wt. %(HC-4) displayed in Table 2. From the ANOVA results, it was observed that the sliding distance is the most dominating factor in wear loss with a contribution of 53.96%. Whereas load is the second dominating factor that plays an important role in the wear loss of specimens. The contribution of the loadwas noticed as 15.43% for HC-4. The third parameter, i.e., sliding velocity, is the least influencing, and the contribution of sliding velocity on wear loss was noticed as 23.72% for HC-4. P-values obtained by ANOVA analysis vary for all controlling parameters; the p-value also indicates the significance of the parameter. The lesser p-value indicates the parameter is most significant and vice versa.

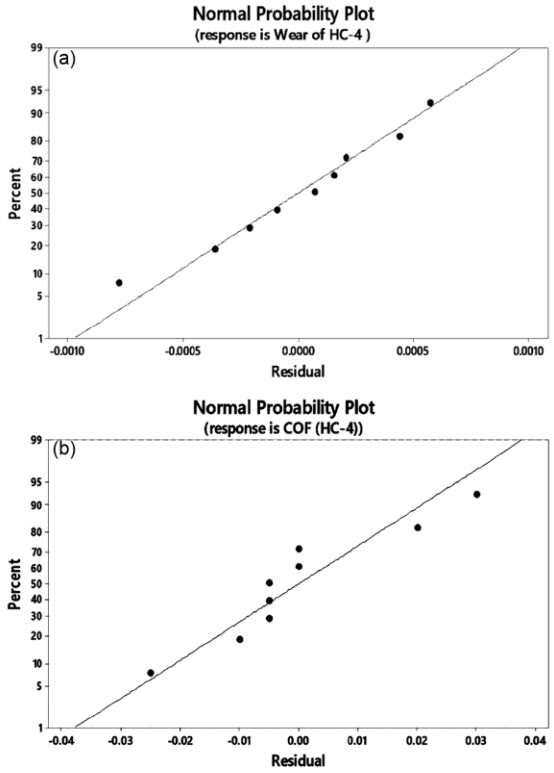

Fig. 5 — Normal probability plots for (a) wear, and (b) Coefficient of Friction (COF).

3.5 Effect of reinforcement on COF

The effect of nano Si_3N_4 reinforcement incorporation in AA 7068 alloy with its increasing content for each experiment is displayed in Table 3. The average values of COF for HC-1, HC-2, HC-3, and HC-4 are 0.0471, 0.456, 0.0432, and 0.0420, respectively. The average percentage reduction in COF for HC-2, HC-3, and HC-4 are 3.18, 8.28, and 10.82 % compared to HC-1. The reduction in COF with increasing wt. % credited to the remarkable properties of Si_3N_4 ceramic particles; these are very hard with excellent good load-bearing capacity. When these hard particles are embedded in a soft alloy matrix, composites' overall load-bearing capacity and tribological properties are enhanced [20, 21]. The anti-friction capability of HC-4 is higher than alloy and

Table 2 — ANOVA for sliding wear of HC-4

Source	DF	Seq SS	Contribution	Adj SS	Adj MS	F-Value	P-Value
SV (m/s)	2	0.000000	23.72%	0.000000	0.000000	3.45	0.225
L (N)	2	0.000000	15.43%	0.000000	0.000000	2.24	0.308
D (m)	2	0.000000	53.96%	0.000000	0.000000	7.84	0.113
Error	2	0.000000	6.88%	0.000000	0.000000		
Total	8	0.000000	100.00%				

S=0.0000059 R-sq=93.12% R-sq(adj)=87.48%

Table 3 — ANOVA for frictional coefficient (COF) of HC-4

Source	DF	Seq SS	Contribution	Adj SS	Adj MS	F-Value	P-Value
sliding velocity (m/s)	2	0.023702	16.47%	0.023702	0.011851	3.00	0.250
Load (N)	2	0.104651	72.73%	0.104651	0.052326	13.25	0.070
Rubbing distance (m)	2	0.007634	5.31%	0.007634	0.003817	0.97	0.509
Error	2	0.007899	5.49%	0.007899	0.003949		
Total	8	0.143886	100.00%				

S= 0.0628437 R-sq= 94.51% R-sq(adj)= 88.04%

composites with lower filler content. Si_3N_4 is also sensitive to environmental humidity during the sliding test. It reacts with the atmospheric H_2O and forms a SiO_2 layer between the specimen and the disc. This formed oxide layer acts as a lubricant, resulting in the frictional co-efficient decreasing COF [14]. The wear loss is also affected by the formation of Al_2O_3 and Fe_2O_3 oxides at the contact surface.

3.6 Effect of wear parameters on COF

The main effective plot shows the effect of operating variables on COF for Al 7068 alloy and nanocomposites (Fig. 4 (b)). By increasing the load on the pin coefficient of friction is reduced for all compositions, this wear behaviour might be due to the formation of Al_2O_3 and Fe_2O_3 tribo- chemical layers in the case of Al 7068alloy and additional SiO_2 layer for nanocomposites. These layers are oxide layers and behave like solid lubricants, resulting in COF decreasing. Similarly, by the increasing sliding velocity, COF reduced, the decrement in COF might be attributed to the MML formation between the specimen and hard surface. The thickness of MML increases with velocity increment resulting ina reduction of COF [22,14]. The effect of Sliding distance (800, 1600, and 2400m) on COF is shown in fig. 4 (b). It is noticed that COF increased with the increase in sliding distance. The variation in COF values is smaller, but an increasing trend due to the strong chemical layer vanished after covering some distance resulting in increased frictional force. The percentage contribution of load, sliding velocity, and rubbing distance on COF is shown in the analysis of variance Table 3.

From the ANOVA results, the load has the most influential parameter, which contributions for HC-4is 72.73%. Whereas sliding/rubbing velocity is the second most impactful parameter on COF, the contribution of sliding velocity for HC-4 is 16.47%.The effect of sliding distance on COF is the least compared to others; the percentage contribution of sliding/rubbing distance for HC-4is5.31%. P-value also confirms the significance of each parameter. From the ANOVA table for COF of HC-4, a lower p-value was obtained for load, indicatingthe most significant parameter compared to others. Similarly, the p-value increases for sliding velocity and rubbing distance, which shows that these are less significant than load.

3.7 Regression analysis

Regression analysis is done for COF and sliding wear using the DOE technique in Minitab 18.1 software for all compositions (HC-1, HC-2, HC-3, and HC-4) by considering sliding velocity, load, and rubbing distance as continuous factors. Normal probability (NP) plots for wear loss and COF generated by the regression tool show the acceptability of regression model equations. A 95% confidence level was considered to predictwear loss and COF. NP plots for sliding wear and frictional coefficient are shown in Fig. 5 (a, and b), respectively. Referring to the figures, all the response values are very close to a straight line, proving the adequacy of regression modelling [23]. R square values for wear loss of HC-4 is 93.12%. Similarly, the variation in adjacent R-value for HC-4 is 87.48%, that shows the variation in the wear loss in percentage. Likewise, the adjacent R-value for COF for HC-4 is 88.04%. The obtained results show that adjacent values for wear loss and COF are above 80%, showing significant variation in measured values obtained from experimentation.

3.8 Worn surface analysis

The SEM images of the worn-out surface of HC-1, HC-2, HC-3, and HC-4 at the maximum level of sliding velocity (3.141m/s), sliding distance (2400m) and load (45N) are shown in Fig. 6. It is noticed that shallow grooves, more material flow, and raptured surfaces are presented in the worn image of HC-1. Adhesive and abrasive wear traces are found in the analysis of worn surfaces. The removal of material is majorly due toplastic deformation. At higher sliding velocity, the surface wears due to the ploughing actions by fragmented matrix and reinforcement particles. A deeper scratch line is found in the case of HC-1, while as the reinforcement % increases, undipped grooves are formed during sliding wear. Composite became more resistant to wear when there was a more reinforcing particle in the matrix. The undipped scratch line was found in micrographs of HC-4 due to higher reinforcement. The presence of a hard phase increases the load-bearing capacity of the composite. Si_3N_4 particles and wear debris are found at the surface of nanocomposites.

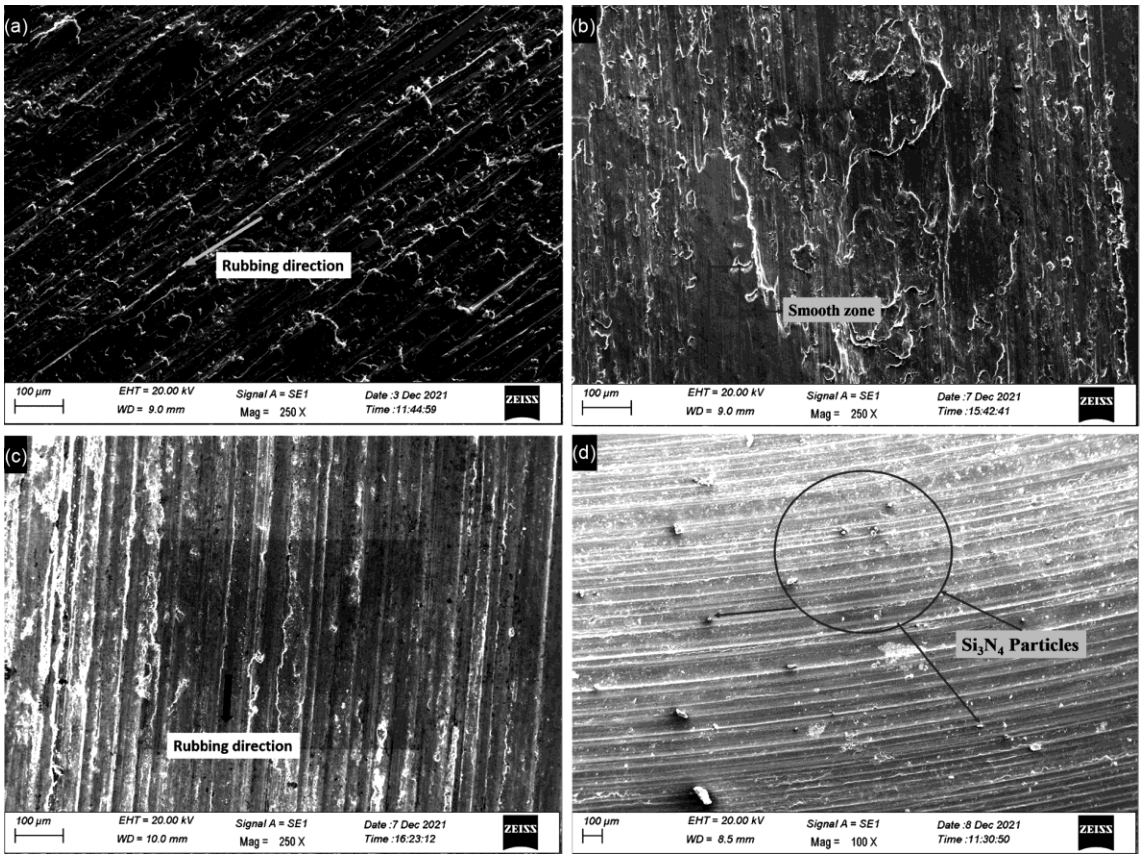

Fig. 6 — Worn-out SEM micrographs at 3.141m/s sliding velocity, 45N load and 2400m rubbing distance (a) HC-1, (b) HC-2, (c) HC-3, and (d) HC-4.

4 Conclusion

The production of Al 7068 alloy-based nanocomposites comprises 0 wt. %. 0.5 wt. %, 1 wt. % and 1.5 wt.% nano Si_3N_4 has successfully been done through stir casting method advanced with ultrasonication techniques, after wear and microstructure study following conclusion drawn from of this research.

- Wear resistance of Al 7068 alloy increases with the inclusion of reinforcement in various wt. %. The decrement in wear loss for HC-2, HC-3, and HC-4 are 13.88%, 27.78%, and 37.5% compared to HC-1.
- Reduction in wear loss found with an increase in sliding velocity due to the formation of tribo-chemical layer at the interface of the pin and hard surface. The increasing trend of wear loss was found with an increase in rubbing distance and load.
- Sliding distance is the most influential factor in wear loss; the contribution of sliding/rubbing distance on wear loss is 53.96% for HC-4.
- The COF is decreased with increasing weight % of Si_3N_4, the average percentage reduction in COF for HC-2, HC-3, and HC-4 are 3.18%, 8.28%, and 10.82% compared to H-1.
- Load is the most dominating factor in frictional co-efficient followed by sliding velocity and rubbing distance; the contribution of Load on COF for HC-4 is 72.73%.

References

1 Joshua K J, Vijay S J & Selvaraj D P, *Ceram. Int,* 44 (2018) 20774.
2 Prasad Reddy A, Vamsi Krishna P, & Rao R N, *Silicon,* 11 (2019) 2853.
3 Wang M, *Mater Sci Eng A,* 590 (2014) 246.
4 Velickovic S, Stojanovic B, Babić M & Bobic I, *J Compos Mater,* 51 (2017) 2505.
5 Zhou J, *Ceram. Int,* 45 (2019) 13308.
6 Suresh S, Gowd G H & Deva Kumar M. L. S, *J Inst Eng Ser D,* 100 (2019) 97.
7 Liu R, Wang W, Chen H, Wan S, Zhang Y, & Yao R, *J Alloys Compd,* 788 (2019) 1056.
8 Xu T, Li G, Xie M, & Liu M, *J Alloys Compd,* 787 (2019) 72.
9 Akbari M K, Baharvandi H R, & Shirvanimoghaddam K, *Mater Des,* 66 (2015) 150.

10 Kumar G B V, Panigrahy P P, Nithika S, Pramod R & Rao C S P, *Compos Part B Eng*, 175 (2019) 107138.
11 Mohanavel V, Ali K S A, Prasath S, Sathish T & Ravichandran M, *J Mater Res Technol*, 9 (2020) 14662.
12 Bhuvanesh D & Radhika N, *J Eng Sci Technol*, 12 (2017) 1295.
13 Raj N & Radhika N, *Silicon*, 11 (2019) 947.
14 Mistry J M & Gohil P P, *Compos Part B Eng*, 161 (2019) 190.
15 Sharma N, Khanna R, Singh G & Kumar V, *Part Sci Technol*, 35 (2017) 731.
16 Stalin B, Ramesh Kumar P, Ravichandran M, Siva Kumar M & Meignanamoorthy M, *Mater Res Express*, 6 (2019) 286.
17 Alipour M & Eslami-Farsani R, *Mater Sci Eng A*, 706 (2017) 71.
18 Diler E A & Ipek R, *Compos Part B Eng*, 50 (2013) 371.
19 Ramesh C S, Keshavamurthy R, Channabasappa B H & Pramod S, *Tribol Int*, 43 (2010) 623.
20 Archard J F, *J Appl Phys*, 24 (1953) 981.
21 Ramesh C S, Keshavamurthy R, Channabasappa B H & Ahmed A, *Mater Sci Eng A*, 502 (2009) 99.
22 Baradeswaran A & Elaya Perumal A, *Compos Part B Eng*, 54 (2013) 146.
23 Ravindran P, Manisekar K, Narayanasamy P, Selvakumar N & Narayanasamy R, *Mater Des*, 39 (2012) 42.